Biochimica et Biophysica Acta 1828 (2013) 1293–1301

Contents lists available at SciVerse ScienceDirect

Biochimica et Biophysica Acta

journal homepage: www.elsevier.com/locate/bbamem

Optimising the combination of thermostabilising mutations in the neurotensin receptor for structure determination

Yoko Shibata [a,1], Jelena Gvozdenovic-Jeremic [b,2], James Love [c,3], Brian Kloss [c], Jim F. White [b], Reinhard Grisshammer [b,*], Christopher G. Tate [a,*]

[a] MRC Laboratory of Molecular Biology, Hills Road, Cambridge CB2 0QH, UK
[b] Membrane Protein Structure Function Unit, National Institute of Neurological Disorders and Stroke, National Institutes of Health, Department of Health and Human Services, Rockville, MD 20852, USA
[c] Protein Production Facility of the New York Consortium on Membrane Protein Structure, New York Structural Biology Center, New York 10027, NY, USA

ARTICLE INFO

Article history:
Received 12 October 2012
Received in revised form 7 January 2013
Accepted 9 January 2013
Available online 18 January 2013

Keywords:
Neurotensin receptor
Thermostability
Membrane protein
Structure

ABSTRACT

Conformational thermostabilisation of G protein-coupled receptors is a successful approach for their structure determination. We have recently determined the structure of a thermostabilised neurotensin receptor NTS1 in complex with its peptide agonist and here we describe the strategy for the identification and combination of the 6 thermostabilising mutations essential for crystallisation. First, thermostability assays were performed on a panel of 340 detergent-solubilised Ala/Leu NTS1 mutants and the best 16 thermostabilising mutations were identified. These mutations were combined pair-wise in nearly all combinations (119 out of a possible 120 combinations) and each mutant was expressed and its thermostability was experimentally determined. A theoretical stability score was calculated from the sum of the stabilities measured for each double mutant and applied to develop 24 triple mutants, which in turn led to the construction of 14 quadruple mutants. Use of the thermostability data for the double mutants to predict further mutant combinations resulted in a greater percentage of the triple and quadruple mutants showing improved thermostability than if only the thermostability data for the single mutations was considered. The best quadruple mutant (NTS1-Nag36k) was further improved by including an additional 2 mutations (resulting in NTS1-GW5) that were identified from a complete Ala/Leu scan of Nag36k by testing the thermostability of the mutants *in situ* in whole bacteria. NTS1-GW5 had excellent stability in short chain detergents and could be readily purified as a homogenous sample that ultimately allowed crystallisation and structure determination.

1. Introduction

The rate of structure determination of G protein-coupled receptors (GPCRs) has dramatically increased over the last 5 years. Initially, only bovine rhodopsin yielded crystals sufficiently well-ordered to allow high-resolution structures to be solved [1–4], but as of August 2012, the structures of 15 other GPCRs have been determined, in complex with agonists, antagonists, antibodies, and/or heterotrimeric G protein [5]. One of the key factors that allowed their crystallisation was the development of techniques that stabilise the receptor either during the crystallisation process or from an earlier stage by direct thermostabilisation of the receptor in a specific conformation [6–8]. If the GPCR is stabilised by a tightly-bound ligand that locks it in a single conformation, then crystallisation of GPCR fusion proteins is possible in cholesterol-rich lipidic cubic phase, with the cholesterol providing additional stability to the receptor [9]. This strategy has proven successful for both aminergic and peptidergic receptors such as the β_2-adrenergic receptor (β_2AR) [10], the adenosine A_{2A} receptor (A_{2A}R) [11], and the opioid receptors [12–15]. In contrast, addition of thermostabilising mutations, but not gene fusions, was essential for the crystallisation of β_1AR and A_{2A}R in highly destabilising detergents such as octylthioglucoside, Hega-10 or nonylglucoside [16–21]. Thermostabilisation of a GPCR in the presence of an agonist or antagonist changes the equilibrium between the different conformations of the receptor, resulting in the stabilisation of either an agonist-bound state or an antagonist-bound state [19,22–24]. When this is performed on the same receptor, then the mutations that stabilise each conformation are quite distinct with only a small overlapping population that stabilises the receptor in both conformations [23]. The advantage of using thermostabilised receptors for crystallisation is that they are stabilised preferentially in a single conformation and this allows structure determination in a complex with low-affinity ligands that do not themselves significantly stabilise the receptor, such as the

* Corresponding authors. Tel.: +44 1223 402266.
E-mail addresses: reinhardg@helix.nih.gov (R. Grisshammer), cgt@mrc-lmb.cam.ac.uk (C.G. Tate).
[1] Current address: MedImmune, Milstein Building, Granta Park, Cambridge CB21 6GH, UK.
[2] Current address: National Human Genome Research Institute, National Institutes of Health, Department of Health and Human Services, Bethesda, Maryland 20892, USA.
[3] Current address: Albert Einstein College of Medicine, Price Center, New York 10461, NY, USA.

0005-2736/$ – see front matter © 2013 Elsevier B.V. All rights reserved.
http://dx.doi.org/10.1016/j.bbamem.2013.01.008

agonist-bound structures of β_1AR [18] and the structures of A_{2A}R bound to caffeine [21] or adenosine [16].

Although the advantages of having a thermostabilised GPCR for structural and biophysical analysis are clear, the generation of such mutants is time consuming. It is true that once a thermostabilised receptor is produced the mutations can be transferred *en bloc* to members within the same family [25], resulting in their thermostabilisation, but this does not work for distantly related receptors as is evident from the apparent lack of conservation of the thermostabilising mutations across multiple receptor families. Thus anything that helps the efficient generation of the thermostabilised receptors would be advantageous. We have therefore studied the most difficult step in the thermostabilisation procedure, namely combining the single thermostabilising mutations to make an optimally stable receptor. The target we have chosen for this study is the neurotensin receptor, NTS1 [26]. Previously, we had developed a mutant, NTS1-7m, that was significantly more stable than the wild-type receptor in both the unliganded state and with neurotensin bound [22]. Unfortunately, NTS1-7m had a strong tendency to aggregate upon purification and therefore was unsuitable for crystallisation. This may have been at least partly because we generated an NTS1 mutant that was stable both in the presence and absence of NT, choosing combinations from mutations that stabilised both the unliganded state and the agonist-bound state. In the work described here, we re-designed the screening procedure and made extensive systematic combinations of mutations, which stabilised NTS1 in the agonist-bound form, whilst ignoring mutations that stabilised NTS1 in the unliganded form. The stability of one of the resulting quadruple mutants was further improved by including 2 additional mutations, generating an ultra-stable neurotensin receptor. The structure of thermostablised NTS1 fused to T4 lysozyme was recently determined from material produced in insect cells [27].

2. Materials and methods

2.1. Expression of NTS1 in Escherichia coli

Bacterial expression plasmids encoding the NTS1 fusion proteins consisted of the *E. coli* maltose binding protein (MBP) with its signal peptide, followed by the N-terminally truncated rat NTS1 (starting at T43) and a C-terminal affinity tag [28]. The various expression constructs used in this study are listed in Table 1. The NTS1 fusion proteins were produced in *E. coli* as described [22,28]. Thermostable mutants were harvested (2 ml aliquots) either 24 h (Nag mutants) or 40 h after induction (Nag36k and GW5 derivatives). The name "Nag" of the single, double, triple and quadruple mutants is derived from "NTS1 thermostabilised in an agonist-bound state". All the Nag mutants were made in the same NTS1 background (Table 1), but there are different modifications in the Nag36k and GW5 derivatives used for purification and crystallisation, which therefore have numbers to define the tags and deletions in the construct.

2.2. Thermostability assays in detergent solution

Cell pellets from 2 ml of IPTG-induced bacterial cultures were resuspended in lysis buffer containing DNaseI and lysozyme (freshly prepared in H_2O). After incubation for 15 min on ice, the respective detergents were added to give a final buffer composition of 50 mM Tris–HCl pH 7.4, 200 mM NaCl, 5 mM $MgCl_2$, 0.75 mg/ml lysozyme, 20 μg/ml DNaseI, and detergent in a total volume of 500 μl. Glycerol was included as indicated. The detergent mixtures used are listed in Table S9. The samples were placed on a rotating mixer at 4 °C for 1 h. Cell debris and non-solubilised material were removed by centrifugation and the cleared lysates containing detergent-solubilised NTS1 were tested for thermal stability in the +NT format [22]. For 1-point assays and thermal denaturation curves, the lysates were diluted into assay buffer (TEBB: 50 mM Tris–HCl pH 7.4, 1 mM EDTA, 0.1% BSA, 0.004% bacitracin; or TN buffer: 50 mM Tris–HCl pH 7.4, 200 mM NaCl; see Table S9) containing 10–12 nM [^{3}H]NT and incubated up to 2.5 h on ice to allow [^{3}H]NT binding to NTS1. Samples (120 μl aliquots) were exposed to different temperatures for the indicated amount of time and placed on ice. Separation of receptor–ligand complex from free ligand (100 μl) was achieved by centrifugation-assisted gel filtration (spin assay) using QS-QM minicolumns packed with Sephadex G50 (equilibrated in 50 mM Tris–HCl pH 7.4, 1 mM EDTA, and 0.1% DDM) [22] or Bio-Spin 30 Tris columns (equilibrated with RDB buffer: 50 mM Tris–HCl pH 7.4, 1 mM EDTA, 0.1% DDM, 0.2% CHAPS, and 0.04% CHS). Control reactions on ice were recorded at the start and at the end of each denaturation experiment. The percentage of activity remaining after heat exposure was determined with respect to the unheated control. Data of thermal denaturation curves were analysed by nonlinear regression using a Boltzmann sigmoidal equation in the Prism software. Individual experiments were conducted as single data points.

2.3. Ala/Leu scanning mutagenesis

Wild-type NTS1 was subjected to alanine/leucine scanning mutagenesis where each residue from I61 to T400, spanning all seven TM helices, three intracellular and three extracellular loops, and the proximal half of the C-terminus was mutated to alanine (if the original amino acid was alanine, then it was mutated to leucine) [22]. All 340 single Nag mutants were tested for thermostability in the +NT

Table 1
Bacterial NTS1 expression constructs. SP-MBP, *E. coli* maltose-binding protein (K1-T366) preceded by the MBP signal peptide; TrxA, *E. coli* thioredoxin (S2-A109); ENLYFQS, Tev protease recognition site; N_{10}, deca-asparagine linker; H_{10}, deca-histidine tag; inner loop 3 deletion Δi3, ΔG275-E296; Nag36k, NTS1 with the thermostabilising mutations A86L–E166A–L310A–V360A; GW5, NTS1 with the thermostabilising mutations A86L–E166A–G215A–L310A–F358A–V360A; amino acid residues are abbreviated in the one-letter code. Note that NTS1 starts in all constructs at T43. Construct details such as the presence or absence of ICL3, or the nature of the C-terminal tag are indicated by the number code for the Nag36k and GW5 mutant series, respectively. See references [22] and [28] for additional details of the NTS1(624) wild-type construct.

Construct ID	N-terminal fusion	Linker	ICL3 modification	End of NTS1	C-terminal tag
Wild-type NTS1					
(624)	SP-MBP	GS	None	Y424	AAA-TrxA-GT-H_{10}
All Nag derivatives					
(624)Nag	SP-MBP	GS	None	Y424	AAA-TrxA-GT-H_{10}
Nag36k derivatives (A86L, E166A, L310A, and V360A)					
(624)Nag36k	SP-MBP	GS	none	Y424	AAA-TrxA-GT-H_{10}
(1937B)Nag36k	SP-MBP	GS	Δi3	Y424	AAA TrxA GT H_{10}
(1937A)Nag36k	SP-MBP	GS-N_{10}-ENLYFQS-GS	Δi3	R420	ENLYFQS-NNNNN-GGGSGGGS-EF-TrxA-GT-H_{10}
(2088)Nag36k	SP-MBP	GS-N_{10}-ENLYFQS-GS	Δi3	K396	A-H_{10}-GG
GW5 derivatives (A86L, E166A, G215A, L310A, F358A, and V360A)					
(1937B)GW5	SP-MBP	GS	Δi3	Y424	AAA-TrxA-GT-H_{10}
(2088)GW5	SP-MBP	GS-N_{10}-ENLYFQS-GS	Δi3	K396	A-H_{10}-GG
(2132)GW5	SP-MBP	GS-N_{10}-ENLYFQS-GS	none	K396	A-H_{10}-GG

format in detergent solution (see Table S9), as well as the double, triple and quadruple Nag mutants.

NTS1(1937B)36k was subjected to alanine/leucine scanning mutagenesis from K64 to S373, using in part the robotic platform of the Protein Production Facility of the New York Consortium on Membrane Protein Structure. Individual NTS1 mutants were expressed in *E. coli* and tested for stability in the presence of [^{3}H]NT using a cell-based rather than a detergent-based assay. Specifically, 30 μl of cell suspension was added to 120 μl TEBB buffer (50 mM Tris–HCl pH 7.4, 1 mM EDTA, 0.1% BSA, 0.004% bacitracin) containing 12.5 nM [^{3}H]NT and placed on ice. After 2 h, 120 μl of the mixture was heated for 30 min at 57.5 °C and then quickly returned to ice. Separation of bound from free ligand was achieved by rapid filtration of 100 μl of the mixture through GF/B glass fibre filters (Whatman) pretreated with polyethyleneimine [28]. A sample kept on ice throughout was used as the unheated control. The receptor survival was recorded as a percentage of [^{3}H]NT binding relative to its respective control. The heat test was conducted once for all mutants, and repeated 2–3 times for promising candidates.

2.4. Purification of NTS1(2088)GW5

NTS1(2088)GW5 was expressed in *E. coli* (100 l culture) in a bacterial fermentor as described previously [28]. For the purification, all steps were performed at 4 °C or on ice. *E. coli* cells (200 g) were resuspended in buffer (50 mM Tris pH 7.4, 200 mM NaCl, and 5 mM $MgCl_2$) supplemented with DNase I (final concentration 4 μg/ml), protease inhibitors (leupeptin at 0.5 μg/ml, pepstatin A at 0.5 μg/ml, AEBSF at 100 μM) and NT (5 μM). Cells were lyzed using an Emulsi-flex homogeniser (Avestin, 3 passes at 15 K–20 K psi). After addition of NaCl to a final concentration of 0.5 M, the sample was centrifuged (45Ti rotor, 40,000 rpm, 45 min, 4 °C, Optima L90K, Beckman). The membrane pellet was resuspended in 600 ml of buffer containing NT and receptors were extracted by drop-wise addition of a 5% DM (n-decyl-β-D-maltopyranoside)/0.5% CHS (cholesteryl hemisuccinate) solution. The final volume was 780 ml containing 50 mM Tris–HCl pH 7.4, 30% glycerol, 200 mM NaCl, 1% DM/0.1% CHS and 2.5 μM NT. After 15 min, the sample was sonicated (20 min, Misonix sonicator 3000 with 1/2-inch flat tip, 1 s on, 2 s off, output level 4) and allowed to stir for an additional 20 min. The sample was clarified by centrifugation (45Ti rotor, 40,000 rpm, 1 h, Optima L90K, Beckman), adjusted with imidazole to a final concentration of 20 mM, and then passed through a 0.2 μm filter (Stericup). Next, the sample was loaded at a flow rate of 1 ml/min onto 20 ml Talon resin packed into an XK26 column (GE Healthcare) equilibrated with buffer A (50 mM Tris pH 7.4, 30% glycerol, 200 mM NaCl, 20 mM imidazole, 1 μM NT, 0.1% DM/0.01% CHS). After washing with 10 column volumes of buffer A, NTS1(2088)GW5 was eluted with buffer B (50 mM Tris, pH 7.4, 30% glycerol, 200 mM NaCl, 200 mM imidazole, 1 μM NT, 0.1% DM/0.01% CHS). Fractions containing NTS1(2088)GW5 (13 ml) were pooled and NT (10 μM) was added. The purified NTS1(2088)GW5 fusion protein was incubated with Tev protease (0.25/1 M/M Tev protease/NTS1 fusion protein, 2 h at room temperature), concentrated to 5 ml (YM50 centriprep, 1500 ×*g*, 4 °C) and loaded onto a 16/60 Superdex 200 column equilibrated in 50 mM Tris pH 7.4, 5% glycerol, 500 mM NaCl, 1 mM EDTA, 1 μM NT, 0.25% n-nonyl-β-D-glucoside, 0.02% azide (0.2 ml/min, 1 ml fractions) to separate cleaved NTS1-GW5 from MBP and Tev protease. Selected fractions were analysed by SDS-PAGE and Amido Black analysis.

3. Results

3.1. Identification of thermostabilising point mutations

In our previous work on NTS1 [22], 340 point mutants were constructed throughout the NTS1 cDNA, with each residue changed to either alanine or leucine (if the residue was already an alanine). Two assays were used to test for thermostability. In the −NT assay, mutants were screened by heating detergent-solubilised receptor in the absence of ligand for 30 min, quenched on ice and the amount of remaining functional receptor determined by using a [^{3}H]NT ligand binding assay. The best 137 mutants that showed stability similar to or better than wild-type receptor were then assayed using the +NT assay, where the heating step was performed in the presence of [^{3}H]NT. The best mutants from each assay were then combined to make NTS1-7m [22].

In order to develop an NTS1 mutant with higher thermostability than wild-type NTS1 and with better properties upon purification than NTS1-7m, we reasoned that only a single conformation should be selected for *i.e.* the neurotensin-bound form. Therefore, the thermostability of the NTS1 mutants in the unliganded state was ignored. This meant that 203 mutants, which had not been assayed in the +NT format, now needed to be investigated so this was the first step in this new work. Assays were performed exactly as described previously by solubilising the *E. coli*-expressed receptors in a mixture of dodecylmaltoside (DDM), CHAPS, cholesteryl hemisuccinate (CHS) and glycerol and then heating the unpurified receptors in the presence of NT for 30 min at 37 °C [22]. The amount of each NTS1 mutant remaining was then compared to the amount of the same mutant present in the unheated solubilised control, and the percentage of receptor still active after heating calculated. These data, in combination with the previous thermostability for the other 137 mutants, identified 68 mutants that were of similar or better stability than the wild-type receptor in the presence of NT. These were then re-assayed under more stringent conditions (+NT assay, 30 min at 40 °C) after solubilisation in DDM that contained a lower percentage of glycerol and in the absence of CHAPS and CHS in order to more accurately differentiate the degree of stabilisation (see Materials and methods). The 16 most thermostabilising mutants (Table S1) were then chosen for further work. Of these 16 mutants, 7 had been identified previously as being more stable than wild-type receptor in the +NT assay and at least as stable as wild-type NTS1 in the −NT assay. The remaining 9 mutants were not previously used, because they were all less stable than the wild-type NTS1 in the −NT assay (Fig. 1).

3.2. Construction and analysis of double mutants

There are 120 combinations of pair-wise mutations that are possible from the 16 most thermostable point mutations [16!/(14!*2!)]. All possible combinations were made, except for G306A/L310A, for which the mutagenesis never worked, and these 119 mutants were then expressed and tested for thermostability. A theoretical stability score was determined from the sum of the stabilities of each point mutant present *i.e.* if mutants A and B had experimentally determined stabilities of 150 and 200, respectively, the theoretical score for mutant A + B was 350. In theory, it would have been possible to convert the measured stabilities, which are expressed here as a score relative to a control, to an energetic term, if a few assumptions are made. However, we have opted to leave them unchanged to provide a clear methodology for anyone wishing to repeat this work on other GPCRs. Comparison of the measured stability with the theoretical stability score for all the double mutants (Fig. 2) identified only one double mutant with a stability close to the apparent sum of the stabilities of the single mutants (Q239A + L310A), with the vast majority of the mutants showing stabilities less than the sum of their parts. In fact, even the most stabilising single mutants can sometimes be combined with other stabilising mutants to result in double mutants with thermostabilities considerably less than that of the wild-type NTS1 (Fig. 2). However, the systematic combination of the mutations also identified a considerable number of mutants that were more thermostable than those generated previously [22]. This was likely due partly to the completeness of the data set, but also, perhaps, to the more

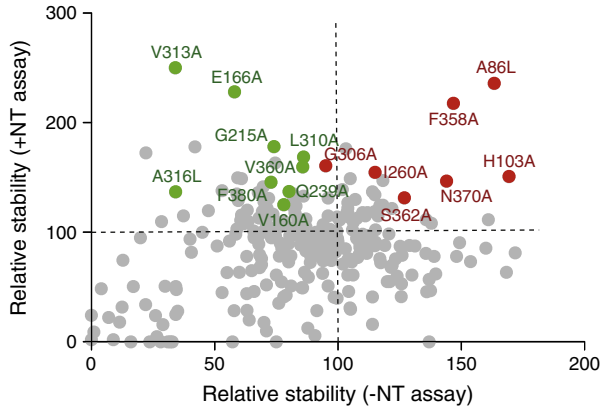

Fig. 1. Stability of NTS1 point mutations. The stability of 340 NTS1 point mutants was determined using the +NT assay [22]. Unpurified *E. coli*-expressed NTS1 fusion protein was solubilised in DDM/CHAPS/CHS and 30% glycerol, incubated with [^{3}H]NT, and half of the sample was heated for 30 min at 37 °C, then quenched on ice. The amount of receptor-bound [^{3}H]NT in the heated sample was compared to the remainder of the sample kept on ice (unheated control). Data for the +NT assay are plotted against the stabilities of the same mutants determined using the −NT assay [22]. The error associated with these measurements is +/− 20%. All measurements were normalised to the stability of wild-type NTS1 (100%). The 68 most stable mutants in the +NT assay were then re-assayed under more stringent conditions (0.13% DDM, 7% glycerol, 40 °C, 30 min, with [^{3}H]NT bound; Table S1); the top 16 mutants are shown coloured and labelled in the scatter plot: red, mutants used previously to derive NTS1-7m [22]; green, new mutants from this study.

important possibility that only a single conformation of receptor was being selected for, which is obviously desirable for crystallisation.

The other factor that needed to be considered was the decrease in functional expression levels upon combination of two stabilising mutations (Table S2). Some pairs of mutations reduced expression levels by over 100-fold which is clearly undesirable for protein production for crystallisation trials. In addition, extremely low levels of functional expression increased the error of the thermostability measurements. For these reasons, only those mutants that expressed above 30 receptors per cell were considered as potentially useful.

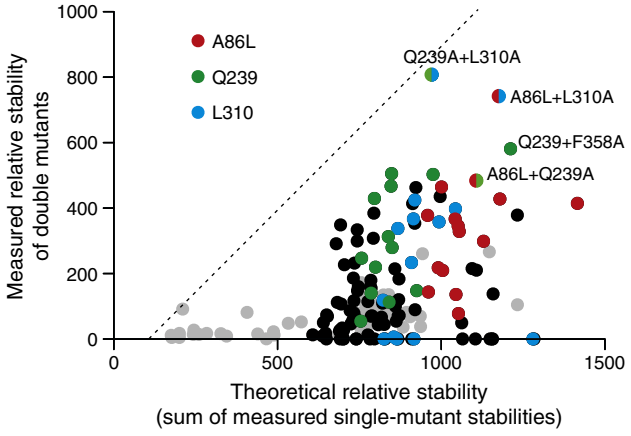

Fig. 2. Stability of NTS1 double mutants. The 119 double mutants were expressed and assayed for stability using the +NT assay (0.13% DDM, 7% glycerol, 47 °C, 30 min, with [^{3}H]NT bound). The measured stabilities are plotted against the theoretical stability determined from the sum of the experimentally determined stabilities of the single mutants. Data for the 119 double mutants made from the 16 most thermostable single mutants are plotted either in black, red (double mutants containing the point mutation A86L), green (double mutants containing the point mutation Q239) or blue (double mutants containing the point mutation L310). Mutants plotted in grey are the double mutants generated during the previous study [22].

3.3. Construction and analysis of triple mutants

If we consider the number of combinations of 3 or 4 point mutants per receptor chosen out of the 16 mutants used to make the double mutants, 560 and 1820 combinations, respectively, there are clearly too many mutants to be made and assayed using the approach described here. Therefore a strategy was devised to reduce the number of combinations that needed to be made. The assumption made was that if mutations A + B, B + C and A + C were all highly additive in the double mutants, then the combination A + B + C would be favourable. In contrast, if any of the 3 double mutants were poorly additive, then it would be less likely that the triple mutant would be highly stabilised. A theoretical score for each of the possible triple mutants was therefore calculated from the sum of the stabilities measured for each of the double mutants represented in the triple mutant. If double mutants showed low [^{3}H]NT binding, they were not included in this analysis. The scores were then sorted and the composition of the theoretical best 16 triple mutants compared (Table S3) and the number of times each single mutant appeared within the list was tabulated. Three mutations (A86L, Q239A and L310A) dominated the list with 10 or more appearances, suggesting that these mutations combined effectively with many different mutations. The next most additive mutations were V160A, A316L and F358A (3 appearances each), with E166A, G215A, G306A, V360A and N370A all appearing once or twice. In contrast, five mutations out of the original 16 (H103A, I260A, V313A, S362A and F380A) did not appear at all in the top 16 theoretical triple mutants, indicating that they were probably not so compatible with other mutations.

All the top scoring 16 theoretical triple mutants were constructed, along with 8 other mutants that included other thermostabilising point mutations, but which were predicted to make slightly less stable triple mutants. Upon measuring the thermostability of the 24 triple mutants constructed, 14 out of the top predicted 16 had stabilities at least 2.5 times greater (±10% error) than the standard chosen for this particular assay (Nag22d), whereas only one out of the other 8 mutants (Nag35f) was this stable (Fig. 3). The Nag35f mutant contained the favourable Q239A + L310A mutations. Out of 53 triple mutants constructed in the previous study [22] only 4 were more stable than Nag22d. Comparison of the measured stabilities of the triple mutants with the theoretical scores, based upon the sum of stabilities of the double mutants, showed a better correlation than was observed for the double mutants (Figs. 3). However, the correlation was still not perfect ($r^2 = 0.44$), necessitating the construction and assaying of multiple mutants to ensure the optimal combination was found.

The apparent denaturation temperature (T_m) of 11 triple mutants was determined after solubilisation in decylmaltoside (Table S3), which is a slightly harsher detergent than dodecylmaltoside. The most stable triple mutant was Nag34a that contained the mutations A86L + L310A + Q239A and had an apparent T_m value of 47 °C. All the other mutants tested had T_m values between 43 and 45 °C, although the order was different from that predicted from the theoretical triple mutant scores.

3.4. Construction and analysis of quadruple mutants

Quadruple mutants were designed by adding the extra mutation selected from V160A, E166A, G215A, A316L, F358A or V360A to each of the 4 best triple mutants Nag34a, 34j, 34l, and 34o based on the apparent T_m measured in DM. Fourteen quadruple mutants were synthesised and tested for stability in comparison to Nag34a (Fig. 4 and Table S4). In order to make the assay more discriminatory, assays were performed on octylglucoside-solubilised receptors heated for 1 h in the presence of [^{3}H]NT. Out of the fourteen mutants tested, 13 were more stable than the best triple mutant Nag34a. Three of the quadruple mutants (Nag36b, 36 k and 36q) were all over 2.5

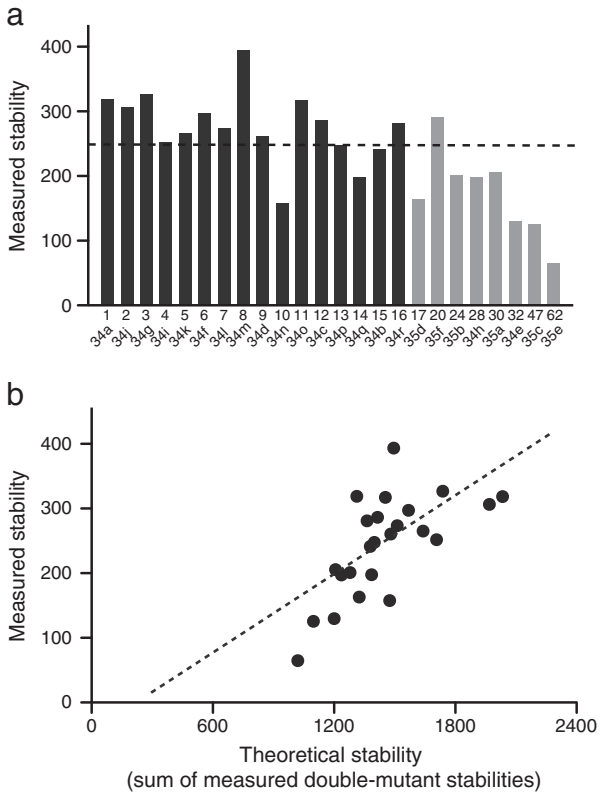

Fig. 3. Stability of NTS1 triple mutants. (a) Twenty-four triple mutants were constructed and assayed for stability using the +NT assay (0.3% DM, 7% glycerol, 45 °C, 30 min, with [^{3}H]NT bound), which included the top 16 stable mutants (black bars) as predicted from the sum of the measured stabilities of the three double mutants composing each triple mutant. Other mutants tested (grey bars) are also shown. Stabilities were normalised against the double mutant NTS1-22d (A86L/Q239A). The number beneath each bar refers to the theoretical rank order position for each mutant. The point mutations in each mutant are shown in Table S3. (b) Correlation between the measured stability of triple mutants compared to their theoretical stabilities ($r^2 = 0.44$; no constraints applied).

times more stable than Nag34a and all of them had an apparent T_m in octylglucoside of 29 °C. One mutant did not express.

3.5. Identification of additional thermostabilisation mutations in Nag36k

The defined end-point for thermostabilisation of GPCRs is when the receptor is sufficiently stable to form well-ordered crystals that diffract well enough to allow structure determination. However, it is clear that further stabilisation of an already thermostabilised receptor is feasible [29,30] and also desirable, because better quality crystals may be produced from more stable proteins. Therefore, whilst Nag36k was being expressed and purified, further stabilisation of the mutant was performed by subjecting the most stable quadruple mutant Nag36k to alanine scanning mutagenesis in the +NT format. The original Ala/Leu scan was performed on an N-terminally truncated version of NTS1 [22], but this scan used the Nag36k derivative NTS1(1937B)36k (Table 1) that had most of the assumed flexible portion of ICL3 removed to aid crystallisation. The thermostability assay was simplified by using *E. coli* cells rather than detergent-solubilised receptors (Fig. 5). Although such an assay will select for NTS1 mutants with improved stability in a lipid environment, we anticipated a parallel improvement in stability of the detergent-solubilised receptor (see below). The top 12 most stabilising mutations identified by Ala/Leu scanning mutagenesis (Table S5) contained 4 mutations (G215A, Q239A, F358A, and S362A) that were previously identified using the +NT format (see Table S1) and 8 mutations that were new. Of particular interest was the mutation F358A, which had previously been identified as thermostabilising in both the +NT and −NT thermostability assays [22]. Although this mutation was not included in the three best quadruple mutants (Nag36b, Nag36k, and Nag36q), F358A conferred the largest stability increase to Nag36k (Table S5). The F358A mutant in wild-type NTS1 background has been found to be constitutively active [31] and in combination with E166A and L310A may have directly promoted an active-like state of NTS1 [27]. Selected mutations, including F358A were combined to generate the mutants GW1-GW6 (Table S6) and NTS1-GW5 was found to be most stable, increasing the thermostability of NTS1-36k by ~4 °C (Table S7). Of interest, the expression levels of all the GW1–GW6 mutants remained at a similarly high level to the NTS1-36k (Tables S5 and S6).

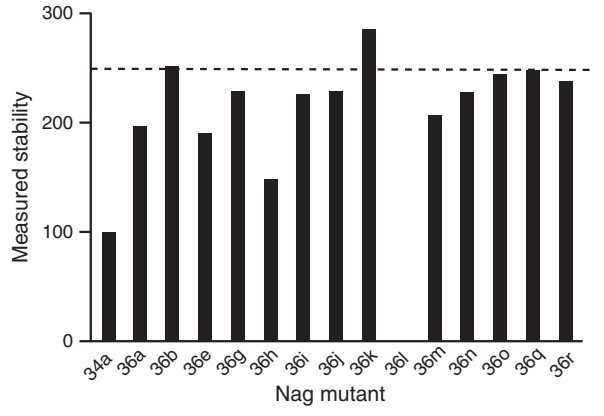

Fig. 4. Stability of NTS1 quadruple mutants. Fourteen quadruple mutants were constructed and their stability determined (0.8% OG, 45 °C, 1 h, with [^{3}H]NT bound). The stabilities were normalised against the stability of NTS1-34a (100%). The dotted line represents 2.5-fold improvement in stability compared to NTS1-34a.

3.6. Biochemical characterisation of NTS1-GW5

NTS1(1937B)GW5 (see Table 1 for nomenclature) contains the 6 thermostabilising mutations A86L$^{1.54}$, E166A$^{3.49}$, G215A^{ECL2}, L310A$^{6.37}$, F358A$^{7.42}$ and V360A$^{7.44}$ (superscripts are the Ballesteros–Weinstein numbers [32]) that are located in the NTS1 transmembrane bundle (except G215A which is located in ECL2). Hence the stabilising effect is likely to reflect the properties of the receptor transmembrane core, but the exact sequence context at the N- or C-termini of NTS1 might also

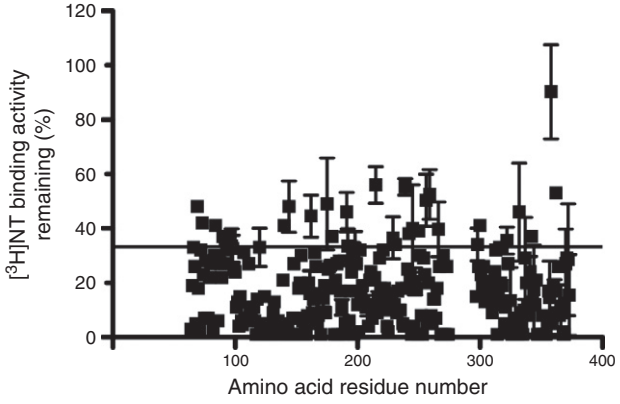

Fig. 5. Stability of 288 mutants generated by Ala/Leu scanning mutagenesis of NTS1(1937B)36k. The NTS1 fusion protein containing 4 thermostabilising mutations was subjected to Ala/Leu scanning mutagenesis. Each of the 288 mutants was expressed in *E. coli*, the cells incubated with the agonist [^{3}H]NT and then heated at 57.5 °C for 30 min (+NT stability test). Receptor survival was recorded as a percentage of [^{3}H]NT binding relative to its unheated control. The horizontal line denotes the remaining activity of NTS1(1937B)36k after heating (33%±2% SE). Error bars (SD) for selected repeat experiments are shown (n=2–4). The x-axis gives the position of the mutated amino acid residues in NTS1.

influence receptor stability. Therefore, we compared the construct NTS1(2088)GW5 (Table 1) with NTS1(1937B)GW5, exploring the effect of the C-terminal TrxA-H_{10} module and the lack of a linker between MBP and NTS1 on the overall receptor stability. We found no difference in stability between these NTS1 constructs (Fig. 6). This suggests that the gain in stability was a reflection of the properties of the transmembrane bundle and that adjacent sequences did not contribute to stabilisation. In addition, the presence or absence of ICL3 did not change the stability of the thermostabilised receptor (compare NTS1(2088)GW5 and NTS1(2132)GW5, Table 1 and Fig. 6). Although NTS1(1937B)GW5 was selected for improved stability in a lipid environment using *E. coli* cells (Tables S5 and S6, Fig. 5), subsequent stability tests in detergent solution (Table S7, Fig. 6) revealed improved stability conferred by the additional G215A and F358A mutations suggesting the use of *E. coli* with the GPCR still in its normal cellular lipid environment as a convenient alternative to detergent-based thermostability assays.

NTS1(1937B)GW5 contains MBP at the receptor N-terminus and the full-length receptor C-terminus followed by the TrxA-H10 tag (Table 1). Such a construct is unlikely to crystallise because of the flexibility of these domains in respect to the NTS1 core. We therefore used NTS1(2088)GW5 for purification, which had a shortened C-terminus and a protease cleavage site between MBP and the receptor. We purified the receptor by immobilised metal affinity chromatography exploiting the C-terminal histidine tag. After incubation with Tev protease and removal of the MBP moiety, the purified cleaved NTS1 showed a symmetrical size exclusion chromatography peak in the detergent n-nonyl-β-D-glucoside (Fig. 7, Table S8) indicating that the species was monodisperse and suitable for crystallisation.

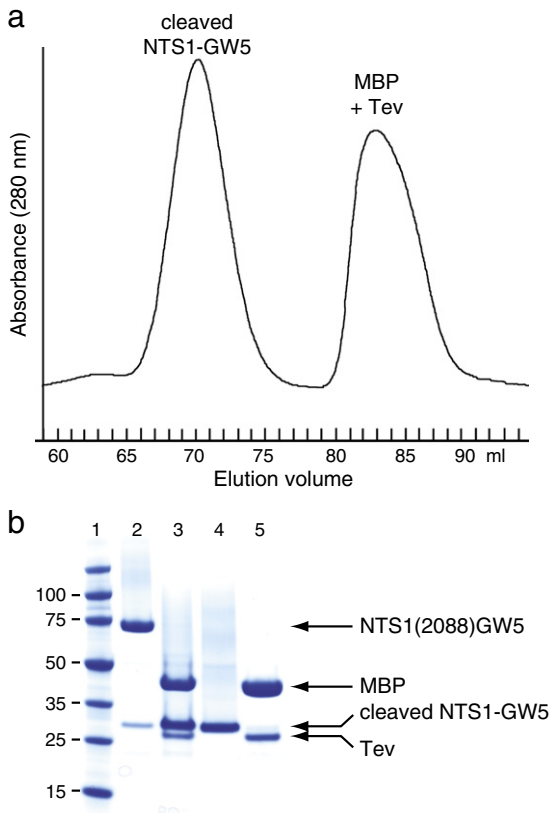

Fig. 7. Purification of NTS1-GW5. The fusion protein NTS1(2088)GW5 was purified by immobilised metal affinity chromatography and incubated with Tev protease to cleave MBP from NTS1. (a) Separation of cleaved NTS1-GW5 from MBP and Tev by size exclusion chromatography. (b) SDS-PAGE gel (NuPAGE 4–12% Bis-Tris gel, Invitrogen, 1× MES SDS buffer, stained with SimplyBlue) analysis of purified fractions: Lane 1, Novagen Perfect Protein Markers (15–150 kDa); lane 2, Talon eluate containing the intact NTS1(2088)GW5 fusion protein; lane 3, Tev protease digest of Talon eluate; lane 4, size exclusion chromatography peak containing purified, cleaved NTS1-GW5; lane 5, size exclusion chromatography peak containing MBP and Tev protease. 5–10 μg protein were loaded per lane. The calculated molecular masses of the NTS1(2088)GW5 fusion protein, cleaved NTS1-GW5, MBP and Tev protease are 81.1 kDa, 38.9 kDa, 42.3 kDa and 28.6 kDa, respectively.

4. Discussion

Thermostabilisation of GPCRs is an effective approach to facilitate their structure determination by X-ray crystallography and for a variety of biophysical assays such as surface plasmon resonance (reviewed in [6]). Currently the fastest and most successful strategy in terms of generating the most thermostable mutant containing the minimum number of mutations is to generate individual point mutations, test their effect on receptor thermostability and then combine 4–6 mutations. This strategy works equally well expressing the mutant receptors in either *E. coli* [22–24,29,33] or in mammalian cells [21], and would also be possible using yeast. Generating ~300 mutants, sequencing them and testing their thermostability are straightforward and can be completed in a few months by an experienced researcher. However, combining the mutations is more problematic given the 8008 combinations of 6 mutations out of a possible 16 [16!/(10!*6!)]. The work presented here describes an exhaustive search for the best 4 mutations out of a possible 16 single mutants (1820 combinations). First, 119 out of a possible total of 120 double mutants were constructed from the 16 most thermostable single mutants and their thermostability determined. What was surprising was the large variation in thermostability of the double mutants, from totally unstable (no [^{3}H]NT binding at 4 °C) to virtually an additive effect between the two mutations. Interestingly, there did not appear to be any mutant that showed a synergistic effect between the two thermostable single mutations. Using the thermostability of these double mutants as a guide, it seemed to be easier to predict which mutations could be combined compared to when only the data from the single mutations were considered, although the correlation between the theoretical stability score and the measured stability was still far from perfect ($r^2 = 0.44$).

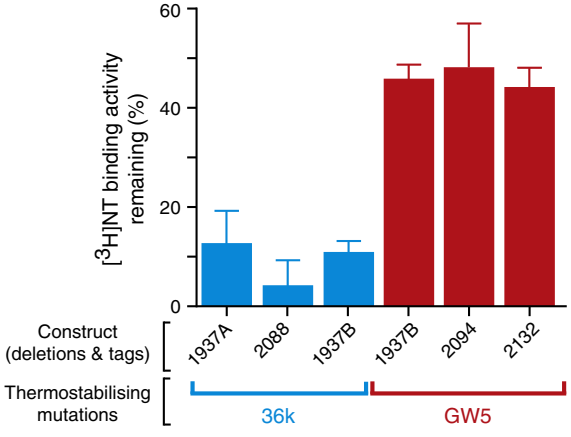

Fig. 6. The stability of NTS1 mutants is not influenced by modifications at the N- and C-termini. DM-solubilised receptors were incubated with the agonist [^{3}H]NT and then exposed to 50 °C for 30 min (+NT stability test). Receptor survival was recorded as a percentage of [^{3}H]NT binding relative to its unheated control. Error bars represent the SD for repeat experiments (n = 2–4).

Of the 14 quadruple mutants constructed 9 showed similar stabilities (within the error of the single-point thermostability assay, ±20%) to the most stable mutant Nag36k, although one quadruple mutant did not fold into a functional receptor. The three best quadruple mutants (Nag36b, 36k, and 36q) all had the same apparent T_m upon solubilisation in OG (28.6 °C, 28.7 °C and 28.8 °C). Thus the systematic methodology produced a number of mutants with equally high thermostability, although this necessitated the construction of 340 single mutants, 119 double mutants, 24 triple mutants and 14 quadruple

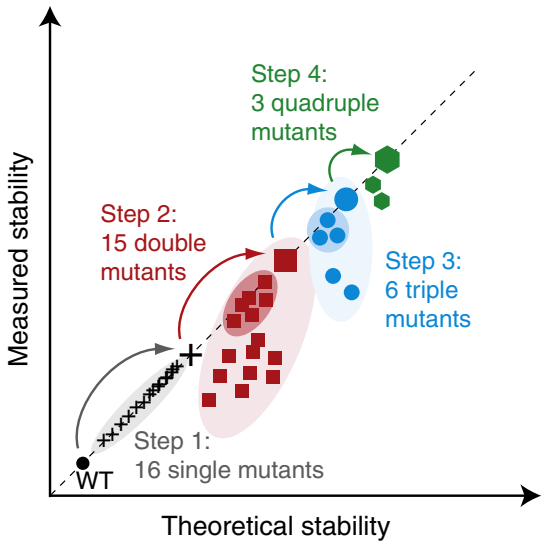

Fig. 8. A simplified strategy for the generation of optimally stable mutants suitable for purification and crystallisation. The graph shows idealised results from the combination of thermostable mutations in a hypothetical receptor, based on the additivity of individual mutations. The dashed line represents mutations that are perfectly additive based on a theoretical score *versus* the actual experimentally determined thermostability (the wild-type and single mutants are placed on this line for clarity, even though it is not possible to predict a theoretical stability). Step 1: The top 16 mutants from an Ala/Leu scan are identified by thermostability assays of the detergent solubilised receptor and the best mutant determined (A). Step 2: Mutant A is combined individually with all the other 15 single mutations (B–P) and the best double mutant determined (A–B). Note that only 6 other mutations are additive to mutant A (mutants C, E, L, M, N, and P) that are close to the dashed line. Step 3: Mutant A–B is combined individually with mutations C, E, L, M, N, and P and the best triple mutant established (A–B–L). Note that only 3 other mutations (E, N, and P) are additive with the double mutant A–B. Step 4: Mutant A–B–L is combined individually with mutations E, N and P and the best quadruple mutant determined (A–B–L–E). Subsequent steps: if time and resources permits, it may be worth combining the optimally stable quadruple mutant with each of the other mutations, but further iterations will probably result in relatively smaller improvements in thermostability. At this stage, if a significant further improvement in thermostability is required, a completely new scanning mutagenesis procedure performed on mutant A–B–L–E may be contemplated, as this has also been shown to be effective in identifying new thermostabilising mutations.

mutants *i.e.* a total of 497 mutants, each of which needed sequencing, expression and determination of stability.

Could the optimally stable quadruple mutants have been obtained without making so many mutants in total? One successful strategy (Fig. 8) that was used on the $A_{2A}R$ (after this work was completed) was to take the most thermostable single mutant, combine it with each of the next 15 most stable mutants and then test their thermostability [24]. The most thermostable double mutant was then combined with the other 14 single mutants (provided they gave good thermostability with the two single mutations in the double mutant) to make a triple mutant and the process repeated to make a quadruple mutant. So, if we had used this process for the thermostabilisation of NTS1, would we have obtained the same thermostable quadruple mutants? From Table S1, it would be apparent that F358A would be the most desirable starting mutation as it is the most thermostable, but its expression is markedly decreased which would reduce its desirability as the 'best' mutation (the receptor has to be purified at some stage for crystallisation). A86L is the next best choice, and if this was taken through the above process using the results from Tables S2, S3 and S4 then the final quadruple mutant would have been A86L–E166A–L310A–V360A *i.e.* Nag36k, one of the three most thermostable quadruple mutants found. This would have involved making only an additional 24 mutations on top of the 340 single mutants originally constructed (Fig. S1). However, the caveat with this gedanken experiment is that some of the combinations of triple mutants (A86L-L310A plus either G306A or H103A) and quadruple mutants (A86L-L310A-V360A plus either A316L or F358A) were untested in this work, so it may have been possible to make an even more thermostable quadruple than Nag36k. If this gedanken experiment is repeated starting with F358A, the most desirable double mutant would have been F358A–A316L, but unfortunately none of the triple mutants constructed in the present work contained this pair of mutations, so further speculation is not possible. However, the evidence available suggests that the systematic combination of mutations as described in Fig. 8 is an efficient and rapid method for obtaining the best thermostable mutant out of a given set of thermostabilising point mutations. To give an idea of the time this would take starting with a new receptor, we estimate that an experienced postdoctoral worker could perform alanine scanning mutagenesis with the thermostability assays and make a stable receptor containing 6 thermostable mutations in about 6 months, providing that the thermostability assay has already been developed.

The quadruple mutant NTS1-Nag36k was further stabilised by performing a complete Ala/Leu scan throughout the receptor and combining two of the mutations to improve the thermostability by an additional 4 °C. The single mutants detected by the screening procedure were interesting from two perspectives. First, the new procedure based upon heating NTS1 mutants in intact *E. coli*, *i.e.* the receptor was in the lipid bilayer rather than in detergent solution, identified 4 thermostabilising mutations that had already been shown to be thermostabilising, including F358A. This validates the methodology, which has the important advantage of being able to process mutants at a very high throughput because the assays use glass fibre filters rather than gel filtration spin columns. Second, 8 new mutations were identified. This has been observed before with both the β_1AR and $A_{2A}R$ where re-scanning through a thermostable mutant identified mutations different from those found in the first screen on the wild-type receptor [21,29]. This is probably to be expected, because the mutated receptors clearly have different properties to the wild-type receptors and therefore different thermostabilising mutations will be needed to stabilise them further. There was insufficient time on this project for an exhaustive trial of different combinations of these new mutations. However, it is evident from the behaviour of the thermostabilised receptor that contains the 6 optimal thermostabilising mutations, NTS1-GW5, that they have conferred sufficient stability for the receptor to be purified as a homogeneous monodisperse preparation in NG, which is a remarkably harsh detergent that cannot be used to purify wild-type NTS1 in a monodisperse state. These results are analogous to the thermostabilisation of the $A_{2A}R$ in an agonist-bound conformation [24], which eventually led to its structure determination at 2.6 Å resolution [16]. Similarly, a construct based on NTS1-GW5 yielded excellent crystals that resulted in its structure being determined to 2.8 Å resolution [27].

The systematic approach we advocate for the identification and combination of thermostabilising mutations is different from the evolution-based methodology proposed by Plückthun and co-workers [34–36]. The basis of their selection procedure is the increase in expression of some thermostable mutants compared to the wild-type receptor, which allows an iterative procedure based on fluorescence-activated cell sorting (FACS) after binding a fluorescent ligand. This does result in improved expression of the receptor in the host cell (*E. coli*) and there is an improvement in thermostability. Of the top 16 thermostable mutations identified in this work (Table S1), only A86L, H103D, I260A and F358A were also identified by FACS-based screening [34,36]. It is also interesting to compare the thermostabilising mutations in NTS1-GW5, which can be purified readily in a monodisperse state in harsh detergents, with NTS1-7m that aggregates badly upon purification and was unsuitable for crystallography [22]. NTS1-7m contained the thermostabilising mutations A86L–I260A–F342A–F358A and NTS1-GW5 contained A86L–E166A–G215A–L310A–F358A–V360A. Both thermostable mutants contained A86L–F358A, but NTS1-7m also contained I260A–F342A that were not included in NTS1-GW5. F342A

was not in the top 16 most thermostable single mutations in the current work and so was not included in the construction of double mutants. I260A was included in the construction of double mutants, but it was found to be poorly additive in comparison with other mutations and therefore it was not used in the construction of the triple mutants.

The differences between the mutations present in NTS1-7m and NTS1-GW5 and their vastly different properties during purification highlights the importance of carefully determining which mutations should be combined. In theory, additional criteria could be included in the screening procedure applied to the mutants to improve the likelihood of obtaining a receptor mutant that does not aggregate. For example, all the mutants could be screened in parallel by fluorescence-detection size exclusion chromatography [37] to exclude those mutants that aggregate in detergent solution. In addition, all the mutants could be screened for their ability to activate G proteins, so that the optimally stable mutant shows wild-type levels of agonist-induced G protein activation, which is not the case for both NTS1 and $A_{2A}R$ stabilised in agonist-bound conformations (see [6] for further discussion). However, both of these strategies would require substantial investment of time and resources during the thermostabilisation procedure. In contrast, the comprehensive data on double mutants presented here showed that it was only necessary to consider those mutations that were most additive to construct a thermostable mutant ideal for crystallisation. A simple rationale for why combining only the additive mutants was successful, is perhaps because they stabilise the same or a very similar 3-dimensional structure of the receptor, although this remains to be tested. Those mutations that were not additive presumably stabilised subtly different conformations and were therefore antagonistic. The simplified strategy presented here for combining point mutations is possible by testing only a small number of mutant combinations and will generate receptor mutants ideal for purification, crystallisation and structure determination.

Contributors

The construction of the single, double, triple and quadruple NTS1 mutants and their stability analysis was done by YS. The concept of conformational thermostabilisation was developed by CGT. The *E. coli* cell-based Ala/Leu scan and subsequent stability tests, resulting in the NTS1-GW mutant series, were performed by JFW and JG-J, with JL and BK collaboratively exploring and performing the automation of alanine scanning mutagenesis. JFW conducted the purification and characterisation of NTS1 mutants. RG was responsible for the overall project strategy towards structure determination. The manuscript was written by RG and CGT.

Acknowledgements

This research was supported by a joint grant from Pfizer Global Research and Development and the MRCT Development Gap Fund in addition to core funding from the UK Medical Research Council MRC U105197215 (YS, CGT) and the Intramural Research Program of the National Institutes of Health, National Institute of Neurological Disorders and Stroke (JFW, JG-J, RG). The Protein Production Facility of the New York Consortium on Membrane Protein Structure was supported by the National Institutes of Health grant U54GM075026 (JL, BK). DNA sequence analysis was performed by the National Institute of Neurological Disorders and Stroke DNA Sequencing Facility.

Appendix A. Supplementary data

Supplementary data to this article can be found online at http://dx.doi.org/10.1016/j.bbamem.2013.01.008.

References

[1] K. Palczewski, T. Kumasaka, T. Hori, C.A. Behnke, H. Motoshima, B.A. Fox, I. Le Trong, D.C. Teller, T. Okada, R.E. Stenkamp, M. Yamamoto, M. Miyano, Crystal structure of rhodopsin: a G protein-coupled receptor, Science 289 (2000) 739–745.
[2] J.H. Park, P. Scheerer, K.P. Hofmann, H.W. Choe, O.P. Ernst, Crystal structure of the ligand-free G-protein-coupled receptor opsin, Nature 454 (2008) 183–187.
[3] P. Scheerer, J.H. Park, P.W. Hildebrand, Y.J. Kim, N. Krauss, H.W. Choe, K.P. Hofmann, O.P. Ernst, Crystal structure of opsin in its G-protein-interacting conformation, Nature 455 (2008) 497–502.
[4] J. Li, P.C. Edwards, M. Burghammer, C. Villa, G.F. Schertler, Structure of bovine rhodopsin in a trigonal crystal form, J. Mol. Biol. 343 (2004) 1409–1438.
[5] M. Audet, M. Bouvier, Restructuring G-protein- coupled receptor activation, Cell 151 (2012) 14–23.
[6] C.G. Tate, A crystal clear solution for determining G-protein-coupled receptor structures, Trends Biochem. Sci. 37 (2012) 343–352.
[7] C.G. Tate, G.F. Schertler, Engineering G protein-coupled receptors to facilitate their structure determination, Curr. Opin. Struct. Biol. 19 (2009) 386–395.
[8] E. Chun, A.A. Thompson, W. Liu, C.B. Roth, M.T. Griffith, V. Katritch, J. Kunken, F. Xu, V. Cherezov, M.A. Hanson, R.C. Stevens, Fusion partner toolchest for the stabilization and crystallization of G protein-coupled receptors, Structure 20 (2012) 967–976.
[9] H.M. Weiss, R. Grisshammer, Purification and characterization of the human adenosine A(2a) receptor functionally expressed in Escherichia coli, Eur. J. Biochem. 269 (2002) 82–92.
[10] V. Cherezov, D.M. Rosenbaum, M.A. Hanson, S.G. Rasmussen, F.S. Thian, T.S. Kobilka, H.J. Choi, P. Kuhn, W.I. Weis, B.K. Kobilka, R.C. Stevens, High-resolution crystal structure of an engineered human beta2-adrenergic G protein-coupled receptor, Science 318 (2007) 1258–1265.
[11] V.P. Jaakola, M.T. Griffith, M.A. Hanson, V. Cherezov, E.Y. Chien, J.R. Lane, A.P. Ijzerman, R.C. Stevens, The 2.6 angstrom crystal structure of a human A2A adenosine receptor bound to an antagonist, Science 322 (2008) 1211–1217.
[12] S. Granier, A. Manglik, A.C. Kruse, T.S. Kobilka, F.S. Thian, W.I. Weis, B.K. Kobilka, Structure of the delta-opioid receptor bound to naltrindole, Nature 485 (2012) 400–404.
[13] A. Manglik, A.C. Kruse, T.S. Kobilka, F.S. Thian, J.M. Mathiesen, R.K. Sunahara, L. Pardo, W.I. Weis, B.K. Kobilka, S. Granier, Crystal structure of the micro-opioid receptor bound to a morphinan antagonist, Nature 485 (2012) 321–326.
[14] A.A. Thompson, W. Liu, E. Chun, V. Katritch, H. Wu, E. Vardy, X.P. Huang, C. Trapella, R. Guerrini, G. Calo, B.L. Roth, V. Cherezov, R.C. Stevens, Structure of the nociceptin/orphanin FQ receptor in complex with a peptide mimetic, Nature 485 (2012) 395–399.
[15] H. Wu, D. Wacker, M. Mileni, V. Katritch, G.W. Han, E. Vardy, W. Liu, A.A. Thompson, X.P. Huang, F.I. Carroll, S.W. Mascarella, R.B. Westkaemper, P.D. Mosier, B.L. Roth, V. Cherezov, R.C. Stevens, Structure of the human kappa-opioid receptor in complex with JDTic, Nature 485 (2012) 327–332.
[16] G. Lebon, T. Warne, P.C. Edwards, K. Bennett, C.J. Langmead, A.G. Leslie, C.G. Tate, Agonist-bound adenosine A2A receptor structures reveal common features of GPCR activation, Nature 474 (2011) 521–525.
[17] T. Warne, P.C. Edwards, A.G. Leslie, C.G. Tate, Crystal structures of a stabilized beta1-adrenoceptor bound to the biased agonists bucindolol and carvedilol, Structure 20 (2012) 841–849.
[18] T. Warne, R. Moukhametzianov, J.G. Baker, R. Nehme, P.C. Edwards, A.G. Leslie, G.F. Schertler, C.G. Tate, The structural basis for agonist and partial agonist action on a beta(1)-adrenergic receptor, Nature 469 (2011) 241–244.
[19] T. Warne, M.J. Serrano-Vega, J.G. Baker, R. Moukhametzianov, P.C. Edwards, R. Henderson, A.G. Leslie, C.G. Tate, G.F. Schertler, Structure of a beta1-adrenergic G-protein-coupled receptor, Nature 454 (2008) 486–491.
[20] M. Congreve, S.P. Andrews, A.S. Dore, K. Hollenstein, E. Hurrell, C.J. Langmead, J.S. Mason, I.W. Ng, B. Tehan, A. Zhukov, M. Weir, F.H. Marshall, Discovery of 1,2,4-triazine derivatives as adenosine A(2A) antagonists using structure based drug design, J. Med. Chem. 55 (2012) 1898–1903.
[21] A.S. Dore, N. Robertson, J.C. Errey, I. Ng, K. Hollenstein, B. Tehan, E. Hurrell, K. Bennett, M. Congreve, F. Magnani, C.G. Tate, M. Weir, F.H. Marshall, Structure of the adenosine A(2A) receptor in complex with ZM241385 and the xanthines XAC and caffeine, Structure 19 (2011) 1283–1293.
[22] Y. Shibata, J.F. White, M.J. Serrano-Vega, F. Magnani, A.L. Aloia, R. Grisshammer, C.G. Tate, Thermostabilization of the neurotensin receptor NTS1, J. Mol. Biol. 390 (2009) 262–277.
[23] F. Magnani, Y. Shibata, M.J. Serrano-Vega, C.G. Tate, Co-evolving stability and conformational homogeneity of the human adenosine A2a receptor, Proc. Natl. Acad. Sci. U. S. A. 105 (2008) 10744–10749.
[24] G. Lebon, K. Bennett, A. Jazayeri, C.G. Tate, Thermostabilisation of an agonist-bound conformation of the human adenosine A(2A) receptor, J. Mol. Biol. 409 (2011) 298–310.
[25] M.J. Serrano-Vega, C.G. Tate, Transferability of thermostabilizing mutations between beta-adrenergic receptors, Mol. Membr. Biol. 26 (2009) 385–396.
[26] K. Tanaka, M. Masu, S. Nakanishi, Structure and functional expression of the cloned rat neurotensin receptor, Neuron 4 (1990) 847–854.
[27] J.F. White, N. Noinaj, Y. Shibata, J. Love, B. Kloss, F. Xu, J. Gvozdenovic-Jeremic, P. Shah, J. Shiloach, C.G. Tate, R. Grisshammer, Structure of the agonist-bound neurotensin receptor, Nature 490 (2012) 508–513.
[28] J.F. White, L.B. Trinh, J. Shiloach, R. Grisshammer, Automated large-scale purification of a G protein-coupled receptor for neurotensin, FEBS Lett. 564 (2004) 289–293.
[29] J.L. Miller, C.G. Tate, Engineering an ultra-thermostable beta(1)-adrenoceptor, J. Mol. Biol. 413 (2011) 628–638.

[30] N. Robertson, A. Jazayeri, J. Errey, A. Baig, E. Hurrell, A. Zhukov, C.J. Langmead, M. Weir, F.H. Marshall, The properties of thermostabilised G protein-coupled receptors (StaRs) and their use in drug discovery, Neuropharmacology 60 (2011) 36–44.
[31] S. Barroso, F. Richard, D. Nicolas-Etheve, P. Kitabgi, C. Labbe-Jullie, Constitutive activation of the neurotensin receptor 1 by mutation of Phe(358) in Helix seven, Br. J. Pharmacol. 135 (2002) 997–1002.
[32] J.A. Ballesteros, H. Weinstein, Integrated methods for the construction of three dimensional models and computational probing of structure function relations in G protein-coupled receptors, Methods Neurosci 25 (1995) 366–428.
[33] M.J. Serrano-Vega, F. Magnani, Y. Shibata, C.G. Tate, Conformational thermostabilization of the beta1-adrenergic receptor in a detergent-resistant form, Proc. Natl. Acad. Sci. U. S. A. 105 (2008) 877–882.
[34] C.A. Sarkar, I. Dodevski, M. Kenig, S. Dudli, A. Mohr, E. Hermans, A. Pluckthun, Directed evolution of a G protein-coupled receptor for expression, stability, and binding selectivity, Proc. Natl. Acad. Sci. U. S. A. 105 (2008) 14808–14813.
[35] I. Dodevski, A. Pluckthun, Evolution of three human GPCRs for higher expression and stability, J. Mol. Biol. 408 (2011) 599–615.
[36] K.M. Schlinkmann, A. Honegger, E. Tureci, K.E. Robison, D. Lipovsek, A. Pluckthun, Critical features for biosynthesis, stability, and functionality of a G protein-coupled receptor uncovered by all-*versus*-all mutations, Proc. Natl. Acad. Sci. U. S. A. 109 (2012) 9810–9815.
[37] T. Kawate, E. Gouaux, Fluorescence-detection size-exclusion chromatography for precrystallization screening of integral membrane proteins, Structure 14 (2006) 673–681.